ChemComm

Accepted Manuscript

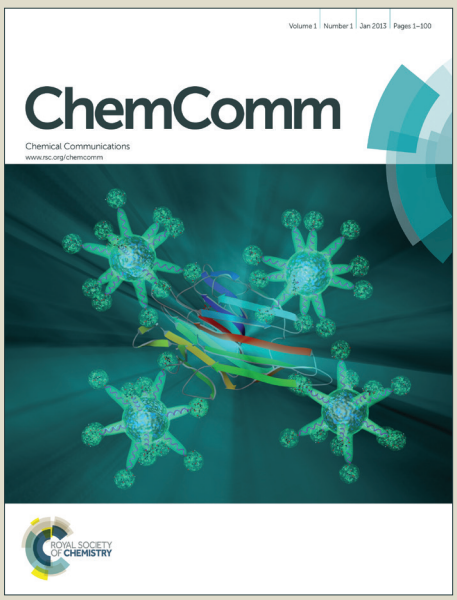

ROYAL SOCIETY OF CHEMISTRY

www.rsc.org/chemcomm

Journal Name

RSCPublishing

COMMUNICATION

High performance and air stable n-type single crystal transistors based on core-tetrachlorinated perylene diimides

Cite this: DOI: 10.1039/x0xx00000x

Received 00th January 2012,
Accepted 00th January 2012

DOI: 10.1039/x0xx00000x

www.rsc.org/

Chunming Liu, Chengyi Xiao, Yan Li,* Wenping Hu, Zhibo Li and Zhaohui Wang*

Organic single crystal transistors based on two kinds of core-tetrachlorinated perylene diimides (4ClPDIs) are fabricated. Compared with alkyl substituted 4ClPDI, the transistors based on fluoroalkyl substituted 4ClPDI exhibit air-stable electron mobility up to 1.43 $cm^2 V^{-1} s^{-1}$ and high photocurrent with an on/off ratio of 1000, which are associated with its closed packing arrangement.

Over the past decade, organic field-effect transistors (OFETs) based on high performance organic semiconductors have received significant attention because of their potential applications in electronics.[1] To this end, a number of organic p-type semiconductors with high hole mobilities have been developed.[2] However, organic n-type semiconductors with high electron mobilities in air condition are still limited because of the lack of good n-type molecular skeletons and insufficient understanding of the structure-property relationship. Organic single crystals are usually regarded as important candidates for the fabrication of high performance devices due to their perfectly ordered molecules, absence of grain boundaries and minimized concentration of charge traps.[3] Thus the single crystal transistors provide an opportunity to reveal the intrinsic structure-property relationship, which provide guidance for the rational design of high performance n-type organic semiconducting materials.

Perylene diimides (PDIs) are regarded as one of the most promising n-type semiconductors due to their accessibility, high electron affinity, and the tunability of optical and electronic properties.[4] Chemical modifications both at imide groups and in bay regions of PDIs are regarded as successful synthetic strategies.[5] Recently, a high-mobility, air-stable n-type organic semiconductor based on core-tetrachlorinated perylene diimide (4ClPDI) was reported, though it has a bad solubility and was purified by consecutive vacuum sublimations due to free NH imide groups.[6] Meanwhile, a new PDI derivative, named C12-4CldiPDI, was also reported by our group, which exhibits excellent n-type transistor behaviour even in air.[7] Considering the accessibility and solubility, herein we focus on the single crystal devices of two different alkyl substituted 4ClPDIs and aim at probing into the influence of different alkyl substitutions to the molecular arrangement and photoelectric performance.

The single crystals of fluoroalkyl and alkyl substituted 4ClPDIs, named C8F-4ClPDI and C8-4ClPDI (Fig. 1a), were grown by the physical vapor transport (PVT) method in a three-zone horizontal-tube furnace. A quartz boat with sample powder was placed in the high temperature zone (220 °C for C8F-4ClPDI and 250 °C for C8-4ClPDI) with high-purity argon used as carrier gas (100 mL/min). Inerratic micrometer-sized crystal ribbons were slowly grown on an octadecyltrichlorosilane (OTS)-modified Si/SiO_2 substrate at a relatively lower-temperature zone. Figure 1b and 1c show low-magnification optical microscopy (OM) images of microribbons and individual crystal scanning electron microscopy (SEM) images. The single-crystal microribbons of both C8F-4ClPDI and C8-4ClPDI exhibit excellent long range regularity with a length of 10 to 100 micrometers and the thickness ranging from several nanometers to tens of nanometers. The surfaces of these microribbons are very smooth and grown in parallel with the substrate.

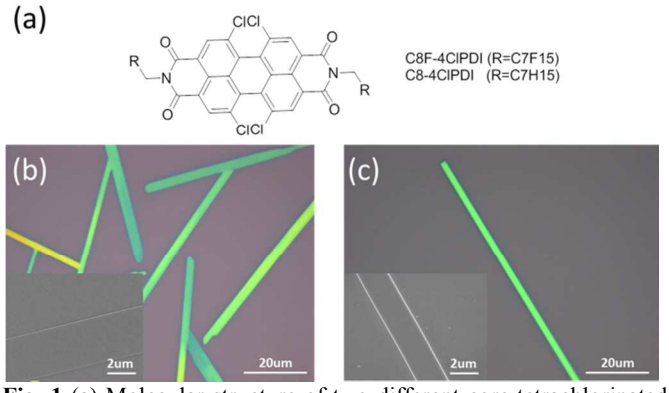

Fig. 1 (a) Molecular structure of two different core-tetrachlorinated perylene diimides. (b) OM and SEM images of single crystal

microribbons of C8F-4ClPDI (c) OM and SEM images of single crystal microribbons of C8-4ClPDI.

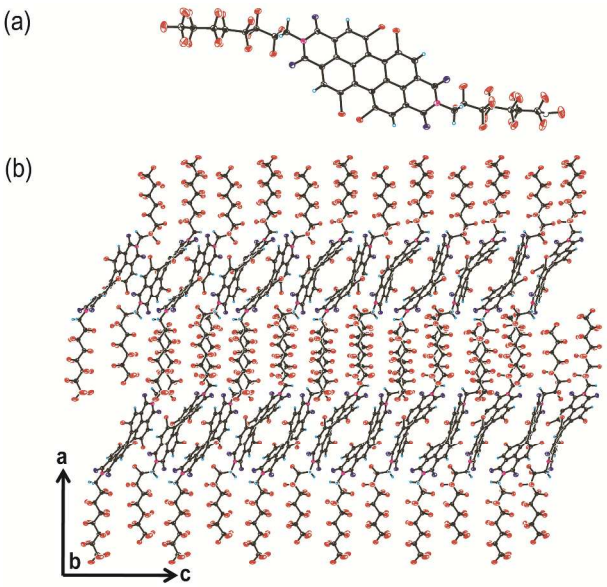

Fig.2 (a) X-ray crystallographic structure of C8F-4ClPDI. (b) Molecular arrangement in the *a*-*c* plane.

For better understanding the molecular arrangement in single-crystal microribbons, crystals suitable for single-crystal X-ray analysis are obtained by slow evaporation of chloroform solution of C8F-4ClPDI. The X-ray data reveal that the crystal of C8F-4ClPDI belongs to the monoclinic crystal system, and the *a*-axis is oriented perpendicularly to the substrate while the *b*–*c* plane (the carrier conduction path) is arranged parallel to the substrate. The crystal structure is shown in Fig. 2a and a highly twisted molecular core can be seen. The crystal packing arrangement are shown in Fig. 2b and Fig. S1, which reveal that the molecules are arranged in columnar stacks along the *c*-axis and lamellar structures along *a*-axis. What should be mentioned is that except the compact stacks during the distorted molecular skeletons, there are many F···F and F···H interactions during the alternately overlapped fluorinated alkyl chains which may effectively prevent the intrusion of H_2O and O_2 in air (Fig. S1, ESI†).

The transmission electron microscopy (TEM) image of a representative single-crystalline microribbon and selected area electron diffraction (SAED) pattern obtained from the same microribbon are shown in Fig. 3a and 3b. The powder X-ray diffraction (XRD) pattern and the atomic force microscopy (AFM) are shown in Fig. 3c and 3d. We can learn from AFM of C8F-4ClPDI that the thickness of each layer of the single crystal microribbons is 20.6 Å, corresponding to the length of the distorted molecular core and a fluorinated alkyl chain. This result is consistent with the XRD data (*d* spacing 20.1 Å) (Fig. 3c). TEM image of C8F-4ClPDI reveals that the single-crystal microribbon exhibits very neat morphology and the corresponding electron diffraction pattern are all show sharp and well-defined diffraction spots (Fig. 3a). AFM and XRD in Fig. 3d demonstrate that the single-crystal microribbon of C8-4ClPDI also takes a lamellar structure, and the thickness of each layer is about 19.3 Å. TEM and SAED images (Fig. 3b) combined with XRD data demonstrate that the single-crystal microribbon of C8-4ClPDI grows along the π-π stacking direction.[8] The well-defined and bright diffraction spots were also found in different regions, proving the single-crystal structure of C8-4ClPDI microribbon.[9] Both compounds of C8F-4ClPDI and C8-4ClPDI can generate highly-crystalline layered structures which may be beneficial to the charge transport in single-crystal microribbons. The XRD Images and SAED patterns of two compounds are very similar. So we speculate that two compounds have a similar molecular arrangement in single-crystal microribbons.

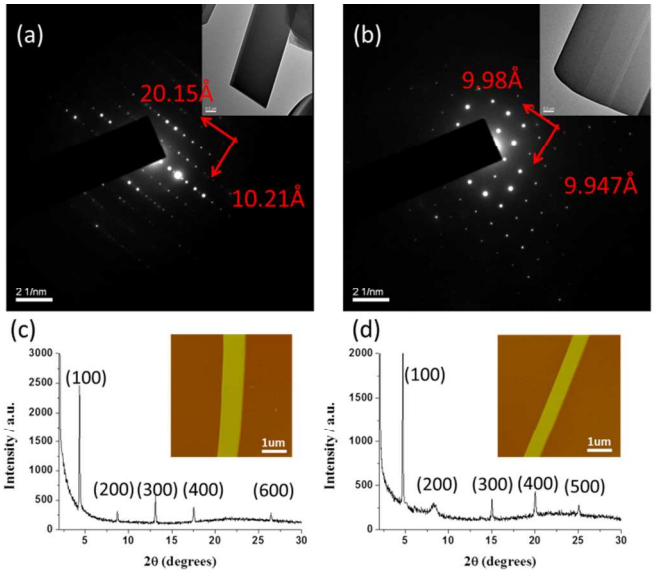

Fig. 3 (a) TEM image of C8F-4ClPDI microribbon and its corresponding SAED pattern. (b) TEM image of C8-4ClPDI microribbon and its corresponding SAED pattern. (c) XRD pattern and AFM image of C8F-4ClPDI single crystal microribbon. (d) XRD pattern and AFM image of C8-4ClPDI single crystal microribbon.

Subsequently, transistors based on single-crystal microribbons of C8F-4ClPDI and C8-4ClPDI were fabricated with doped n-type silicon wafer as the gate electrode, Au as source and drain electrodes, and OTS-modified SiO_2 as the dielectric layer. Firstly, single-crystal microribbons of C8F-4ClPDI or C8-4ClPDI were deposited on an OTS/SiO_2/Si substrate by PVT method. These single-crystal microribbons are all thin enough to minimize the effect of the resistance.[10] Secondly, using our skilful mechanical technique named "pick and paste" method to paste Au electrodes onto crystals directly to avoid the thermal radiation.[11] The OFET devices were fabricated oriented toward the growth direction of single crystal microribbons and all measured under ambient conditions. The transistors based on C8F-4ClPDI exhibit typical n-type semiconducting behavior with the average electron mobility of 1.14 $cm^2 V^{-1} s^{-1}$, the highest electron mobility of 1.43 $cm^2 V^{-1} s^{-1}$, and an on/off ratio of ~ 10^7. Representative output and transfer characteristics of the transistors based on C8F-4ClPDI are plotted in Fig. 4a and 4b. Meanwhile, the anisotropic charge transport in the elongated crystals of C8F-4ClPDI is also explored by using "organic nanowires mask" (Fig. S2, ESI†). It can be seen that the carrier mobility along *c*-axis is far higher than that along *b*-axis, which is attributed to the closed molecular packing arrangement along *c*-axis. For comparison, single-crystal transistors based on C8-4ClPDI exhibit relatively lower mobility along the growth direction with the highest electron mobility of 0.8 $cm^2 V^{-1} s^{-1}$ and an on/off ratio of 10^5. The performance of devices based on C8-4ClPDI attenuated very fast in air. Hence the output curve is unavailable and the transfer characteristics are plotted in Fig. 4d. Considering the different electron mobility and stability of transistors based on

C8F-4ClPDI and C8-4ClPDI, we speculate that the introduction of fluorinated alkyl chains into the imide groups lead to a more close-knit arrangement in the crystal structure. On one hand, this tight arrangement is advantageous for the charge transfer in C8F-4ClPDI based devices.[12] On the other hand, the closely ordered crystal structure against the entrance of water and oxygen molecules in air.[13]

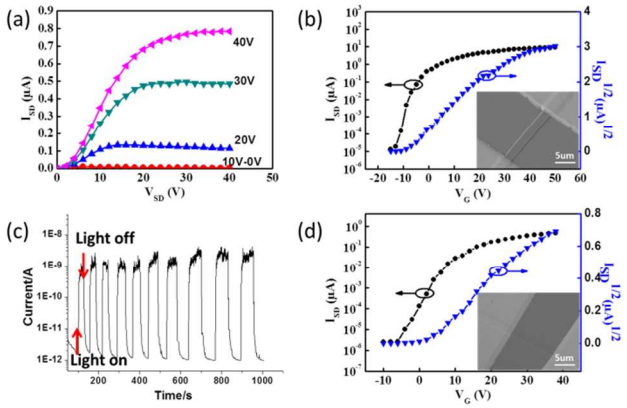

Fig.4 (a) Output and (b) transfer characteristics of the representative single crystal device based on C8F-4ClPDI. Inset shows the SEM image of the single crystal device. (c) Photoresponsive behavior of a two-end single-crystalline device (white light, 3.76 mw/cm^2, an applied bias voltage -10 V). (d) Transfer characteristics of a single crystal device based on C8-4ClPDI. Inset shows the SEM image of the single crystal device.

To further explore the potential applications of C8F-4ClPDI in optoelectronic devices, the optical performance on the switching of white light was performed. The two-end crystal devices based on C8F-4ClPDI were fabricated by "organic nanowire mask" technique in order to make a better contact with the electrode. It was concluded that the single-crystal devices of C8F-4ClPDI exhibit remarkably high sensitivity to light. The current change of the single-crystal devices in the dark and under white light illumination is plotted in Fig.4c and Fig.S4. The photocurrent is found to switch promptly with white light on and off. Moreover, the dark current is only 1.18 × 10^{-12} A. Upon 3.76 mw/cm^2 white light illumination, the photocurrent could approach to 1.52 × 10^{-9} A, indicating an on/off ratio exceed 1000 and an average light responsivity of 2.5 A/W. At the same time, the light response of C8-4ClPDI is bad and the current changes little when the white light is turned on and off.

In summary, organic single-crystal microribbons of two kinds of core-tetrachlorinated perylene diimides are produced by physical vapor transport method, and transistors based on individual crystal are fabricated. Compared with C8-4ClPDI, the transistors based on C8F-4ClPDI exhibit the electron mobility up to 1.43 cm^2 V^{-1} s^{-1} in air and an on/off ratio of 10^7, which are associated with its closed packing arrangement not only during the distorted molecular skeletons but also during the alternately overlapped fluorinated alkyl chains. Moreover, the two-end single-crystal devices based on C8F-4ClPDI show remarkably high sensitivity to light with an on/off ratio of 1000. The comparative results may provide the guidance for the rational design of high performance n-type organic semiconducting materials in the future.

For financial support of this research, we thank the National Natural Science Foundation of China (21204091, 91027043 and 21190032), the 973 Program (2012CB932903), and the Chinese Academy of Sciences (XDB12010100).

Notes and references

Beijing National Laboratory for Molecular Sciences, Key Laboratory of Organic Solids, Institute of Chemistry, Chinese Academy of Sciences, Beijing 100190, P. R. China.
E-mail: wangzhaohui@iccas.ac.cn, yanli@iccas.ac.cn; Fax: +86-10-62653617; Tel: +86-10-62653617

† Electronic Supplementary Information (ESI) available: Intermolecular interaction image, OM image of transistor with four electrodes, statistical mobility distributions, I-V curves, and crystal data for C8F-4ClPDI. See DOI: 10.1039/c000000x/

1 (a) C. Wang, H. Dong, W. Hu, Y. Liu and D. Zhu, *Chem. Rev.*, 2012, **112**, 2208; (b) W. Jiang, Y. Li and Z. Wang, *Chem. Soc. Rev.*, 2013, **42**, 6113; (c) A. N. Sokolov, B. C.-K. Tee, C. J. Bettinger, J. B.-H. Tok and Z. Bao, *Acc. Chem. Res.*, 2012, **45**, 361.

2 (a) M. Gsänger, E. Kirchner, M. Stolte, C. Burschka, V. Stepanenko, J. Pflaum and F. Würthner, *J. Am. Chem. Soc.*, 2014, **136**, 2351; (b) X.-Y. Wang, F.-D. Zhuang, R.-B. Wang, X.-C. Wang, X.-Y. Cao, J.-Y. Wang and J. Pei, *J. Am. Chem. Soc.*, 2014, **136**, 3764.

3 R. W. I. de Boer, M. E. Gershenson, A. F. Morpurgo and V. Podzorov, *Phys. Status Solidi A*, 2004, **201**, 1302.

4 (a) C. Huang, S. Barlow and S. R. Marder, *J. Org. Chem.*, 2011, **76**, 2386; (b) R. Schmidt, J. H. Oh, Y.-S. Sun, M. Deppisch, A.-M. Krause, K. Radacki, H. Braunschweig, M. Könemann, P. Erk, Z. Bao and F. Würthner, *J. Am. Chem. Soc.*, 2009, **131**, 6215.

5 (a) M. Gsänger, J. H. Oh, M. Könemann, H. W. Höffken, A.-M. Krause, Z. Bao and F. Würthner, *Angew. Chem. Int. Ed.*, 2010, **49**, 740; (b) Q. Yan, Y. Zhou, Y.-Q. Zheng, J. Pei and D. Zhao, *Chem. Sci.*, 2013, **4**, 4389; (c) Z. Zhang, T. Lei, Q. Yan, J. Pei and D. Zhao, *Chem. Commun.*, 2013, **49**, 2882; (d) L. Fan, Y. Xu and H. Tian, *Tetrahedron Lett.*, 2005, **46**, 4443.

6 M.-M. Ling, P. Erk, M. Gomez, M. Koenemann, J. Locklin and Z. Bao, *Adv. Mater.*, 2007, **19**, 1123.

7 (a) A. Lv, S. R. Puniredd, J. Zhang, Z. Li, H. Zhu, W. Jiang, H. Dong, Y. He, L. Jiang, Y. Li, W. Pisula, Q. Meng, W. Hu and Z. Wang, *Adv. Mater.*, 2012, **24**, 2626; (b) H. Qian, Z. Wang, W. Yue and D. Zhu, *J. Am. Chem. Soc.*, 2007, **129**, 10664.

8 S. Dong, H. Zhang, L. Yang, M. Bai, Y. Yao, H. Chen, L. Gan, T. Yang, H. Jiang, S. Hou, L. Wan and X. Guo, *Adv. Mater.*, 2012, **24**, 5576.

9 (a) R. Li, W. Hu, Y. Liu and D. Zhu, *Acc. Chem. Res.*, 2010, **43**, 529;(b) H. Usta, A. Facchetti and T. J. Marks, *Acc. Chem. Res.*, 2011, **44**, 501;(c) S. Liu, W. M. Wang, A. L. Briseno, S. C. B. Mannsfeld and Z. Bao, *Adv. Mater.*, 2009, **21**, 1217.

10 A. L. Briseno, R. J. Tseng, M.-M. Ling, E. H. L. Falcao, Y. Yang, F. Wudl and Z. Bao, *Adv. Mater.*, 2006, **18**, 2320.

11 (a) L. Tan, W. Jiang, L. Jiang, S. Jiang, Z. Wang, S. Yan and W. Hu, *Appl. Phys. Lett.*, 2009, **94**, 153306; (b) L. Tan, L. Zhang, X. Jiang, X. Yang, L. Wang, Z. Wang, L. Li, W. Hu, Z. Shuai, L. Li and D. Zhu, *Adv. Funct. Mater.*, 2009, **19**, 272.

12 T. He, M. Stolte and F. Würthner, *Adv. Mater.*, 2013, **25**, 6951.

13 B. A. Jones, A. Facchetti, M. R. Wasielewski and T. J. Marks, *J. Am. Chem. Soc.*, 2007, **129**, 15259.